

1. Introduction

Goals

- evolution of cloud microstructure
- phase transition and droplet growth and freezing mechanism
- warm and cold precipitation formation

Applied Techniques

- Combined measurement of:
- spectral reflections from edges of convective clouds and depolarization
- Retrieval of:

- vertical profiles of the thermodynamic phase
- effective radius (R_{eff}) based on 3D radiative modeling

2. Measurement Setup: LIRAS

(Lidar and Radiation System for cloud profiling)



Tab. 1: Technical Specifications of LIRAS

	Zeiss-Spectrometer	Lidar (Leosphere ALS300)
Wavelength (nm)	350 -2000	355
Spectral resolution (nm)	FWHM _{VIS} ≈ 3 FWHM _{NIR} ≈ 16 $\Delta\lambda_{VIS} \approx 0.8$ $\Delta\lambda_{NIR} \approx 5$	-
Accumulation Time (s)	1	10 -30
Field of View (°)	1	0.014
Polarization	-	Vertical and Parallel
Scanning Device: Angular resolution: 1°		

Fig. 1: Instrumental setup of LIRAS

VIS: visible, NIR: Near InfraRed

3. Methods

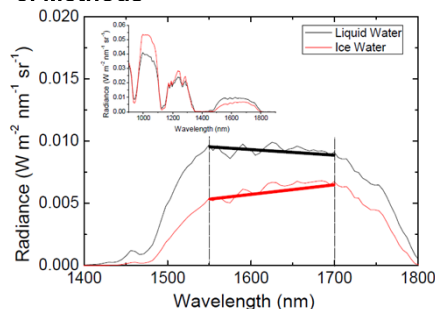


Fig. 2: Measured spectral radiance of cloud edges with ice water cloud particles and liquid water cloud particles in the NIR spectral range

(a) Spectral Slope Method

- spectral slope of radiance I differs for ice and liquid water in the wavelength range of 1.5 -1.7 μm
- ice index: $I_s = \frac{I_{1550 \text{ nm}} - I_{1700 \text{ nm}}}{I_{1700 \text{ nm}}}$
 positive \rightarrow ice
 negative \rightarrow liquid water

(b) Depolarization Method

- linear depolarization ratio δ : ratio of the perpendicular and parallel polarized backscattered intensities
- single scattering approximation: \rightarrow no change of polarization for spherical particles, but depolarization for ice crystals
- multiple scattering increases δ for liquid water clouds with increasing penetration depth: \rightarrow the slope of δ has to be examined

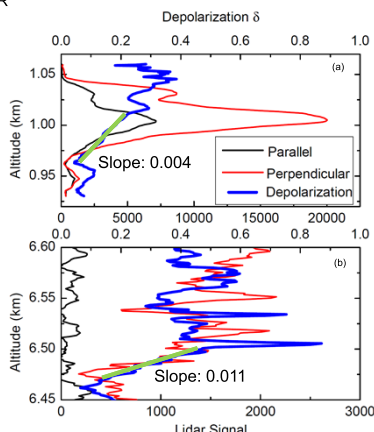


Fig. 3: Lidar signal and depolarization for (a) liquid water cloud and (b) ice cloud.

4. 3D Radiative Transfer Simulations

Monte Carlo Atmospheric Radiative Transfer Simulator



- forward-propagating Monte Carlo photon-transport algorithm

(a) Monodisperse Clouds

- ice indices of clouds with identical microphysical parameters depend significantly on scattering angle

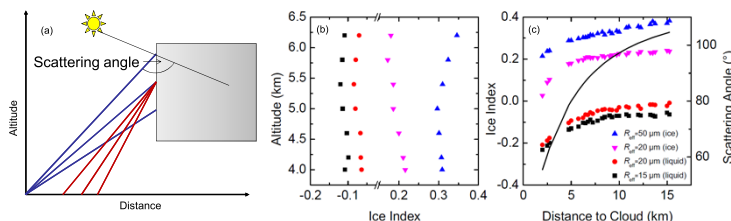


Fig. 4: (a) Viewing geometry, (b) ice index derived from one observing point, (c) ice index of one cloud area, derived from different observing points

(b) Polydisperse Cloud

- clear separation between ice and liquid phase possible, even mixed phase area observable
- small ice particles ($< 20 \mu\text{m}$) might be misinterpreted as liquid particles, because of high SSA (> 0.98)

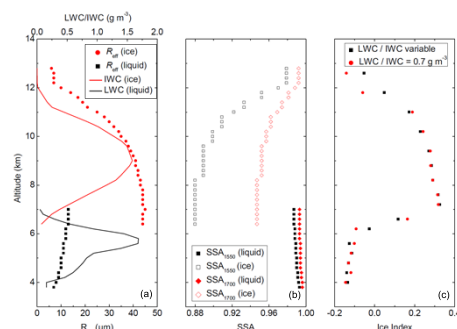


Fig. 5: (a) Vertical profile of R_{eff} and water content, (b) single scattering albedo (SSA), and (c) ice index for one fixed geometry

5. Case Study

- observations of convective cloud field passing Leipzig on June 25th 2012
- measurements taken at altitudes between 0.9 and 2.8 km (geometry information from Lidar data)
- mixed phase (1), ice phase (2) and water phase (4) were observed
- maximum of ice index at (3) results from transmitted radiation of high convective cloud with ice phase which affects spectrum

Tab. 2: Comparison of ice indices and lidar depolarisation slopes; * $R_{eff} = 35 \mu\text{m}$, ** $R_{eff} = 10 \mu\text{m}$

	Mixed Phase (1)	Ice Phase (2)	Liquid Phase (4)
Lidar δ -slope	0.01	0.02	0.005
Ice Index	0.02	0.33	-0.17
Simulated Ice Index	-	0.31*	-0.14**

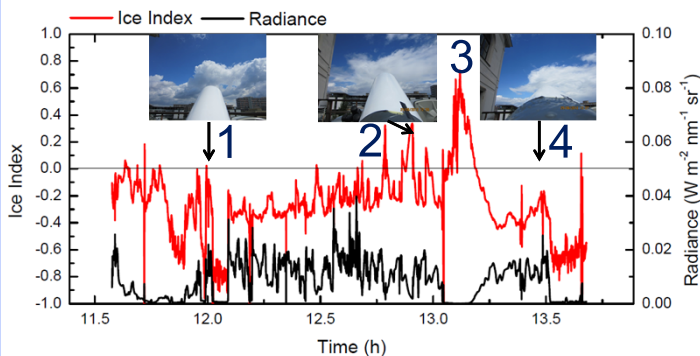


Fig. 6: Time series of spectral radiance at 1550 nm wavelength (black) and derived ice index (red).

6. Outlook



Fig. 7: Zugspitze

- field campaign in September 2012 (Zugspitze)
- in-situ measurements at the summit, remote sensing at Schneefernerhaus
- in addition also R_{eff} retrievals

[1] Pilewskie, P. and Twomey, S., 1987: Discrimination of ice from water in clouds by optical remote sensing, *Atmos. Res.* **21**, 113–122.

[2] Ehrlich, A., E. Bierwirth, M. Wendisch, J.-F. Gayet, G. Mioche, A. Lampert and J. Heintzenberg, 2008: Cloud phase identification of low-level Arctic clouds from airborne spectral radiation measurements. Test of three approaches, *Atmos. Chem. Phys.* **8**, 7493–7505.